Analyzing the Relationship Between Above Ground Biomass and Different Vegetation Indices of Chure Region of Sainamaina Municipality, Nepal

Ananta Poudel[1*], Him Lal Shrestha[1], Niraj Mahat[2], Garima Sharma[1], Sahara Aryal[1], Sujan Kumar Khatri[3]

[1]Kathmandu Forestry College, Kathmandu, Nepal, ,
[2] Institute of Forestry, Tribhuvan University, Hetauda, Nepal
[3] Faculty of Science and Health and Technology, Nepal Open University, Lalitpur, Nepal
**Corresponding author: apoudel816@gmail.com*

ABSTRACT

For REDD+ (reducing emissions from deforestation and forest degradation), sustainable management of forests, and protection and enhancement of forest carbon stocks procedures to be successful, accurate measurement of forest above-ground biomass (AGB) are essential. Sentinel imaging that was launched since 2014 provides an opportunity for mapping and monitoring AGB in forests. The aim of this study is to analyze the relationship between AGB and vegetation indices (VIs) derived from Sentinel-2 imagery in theChure region of Sainamaina municipality. For this, we used 72 sample plots and 7 different VIs. TheARVI(Atmospherically Resistant Vegetation Index) and EVI2 (Enhanced Vegetation Index - 2) shows strong correlation (i.e. r = 0.861 and 0.861) and coefficient of determination value (R2=0.7414 and 0.7415) respectively. Overall, Sentinel-2 multispectral images vegetation indices can produce good results for reporting the AGB.

Keywords: AGB, VIs, Sentinel-2, ARVI, and EVI2

INTRODUCTION

"Forests have a crucial function in reducing CO2 levels in the atmosphere and the global climate system"(Alkama and Cescatti 2016; Pan *et al., 2013*, Nunes et al 2020). As carbon plays a vital part in the earth's carbon cycle, biomass and carbon stock assessment in tropical forests have recently received wider interests(Basuki *et al., 2009*). IN order to quantify the contributions of forests as carbon sources or sinks and to promote sustainable forest management, estimation of forest biomass and carbon stock is crucial. The quantification of forest biomass and carbon stock is crucial in assessing the contributions of forests as carbon sources or sinks and in promoting sustainable forest management practices. (Mauya *et al., 2015*; Temesgen *et al., 2015*)

One way to assess biomass involves a conventional technique that involves destructively measuring aboveground biomass (AGB) by removing trees. While this approach offers relatively accurate results, it is costly and time-consuming due to the need for extensive fieldwork(Attarchi and Gloaguen 2014). The alternative way is to employ a non-destructive technique of data collectionlike Remote Sensing (RS) to estimate biomass from spectrally recorded information (Kumar *et al., 2015*). Due to the accessibility and accuracy of high-resolution images, RS data now plays a crucial role in the calculation of biomass across largepartsof tropical areas(Wahlang & Chaturvedi, 2020). Remote sensing (RS) technology nowadays is a widely used tool for biomass assessment (Kankare *et al., 2013*; Maynard *et al., 2007*; Wannasiri *et al., 2013*). Based on repetitive data gathering with little effort, RS may obtain forest information over broad areas at an affordable price and with satisfactory precision(Lu 2006).

The interpretation of biomass and land cover involves utilizing mathematical transformations of the original spectral reflectance, which are commonly referred to as vegetation indices (VIs)(He et al., 2005; Rahman *et al., 2003*). Satellite-based vegetation indices (VIs) are frequently used in numerous studies to estimate biomass (Foody et al., 2003; Hurcom & Harrison 1998; Li, Zhou, & Xu 2021; Lourenço 2021; Pandit *et al., 2018*; Schlerf *et al., 2005* Sch; Utari *et al., 2020*). Some studies suggest that there exists a noteworthy positive correlation between vegetation indices (VIs) and biomass(Boyd, 1999; Das & Singh 2012; Heiskanen, 2006; Hurcom & Harrison 1998; Steininger, 2000). However, other studies have demonstrated unsatisfactory outcomes(Foody *et al., 2003*; Schlerf *et al., 2005*).

The European Space Agency's Copernicus program was launched in 2014 with additional significant advancements in radiometric, geographical, and temporal resolution to the global repository of open access data (Astola *et al., 2019*; Li *et al., 2021*). For instance, the operational actors notice a significant difference when the spatial resolution is increased from 30 m of Landsat 8 to 10 m of Sentinel-2, which permits calculation of variables (such AGB per ha) at the lower scale levels of forest plots and stands. In comparison to Landsat-8, Sentinel-2 (especially A and B) includes more spectral bands, including three Vegetation Red Edge (VRE) and one Narrow Near Infrared (NNIR) band (13 Sentinel-2 vs. 7 bands) (Biswas et al. 2020; Forkuor *et al., 2017*). It is anticipated that the VRE bands will help with better AGB estimation and mapping(Qiu et al., 2017).

Limited research has been undertaken in Nepal regarding the utilization of remote sensing (RS) technologies, particularly in estimating aboveground biomass (AGB)with few detailed ground-based quantifications of biomass. There is paucity of knowledge on forest biomass in the Chure region due to its geological fragility to undertake destructive methods. Further, application of satellite data with ground data is yet at early stage in Nepal and Cure region is not an exception. Thus, the goal of this study is to analyze the relationship between AGB and different VIs (derived from Sentinel-2 images) of forest of Chure region, Nepal

MATERIALS AND METHODS

Study area:

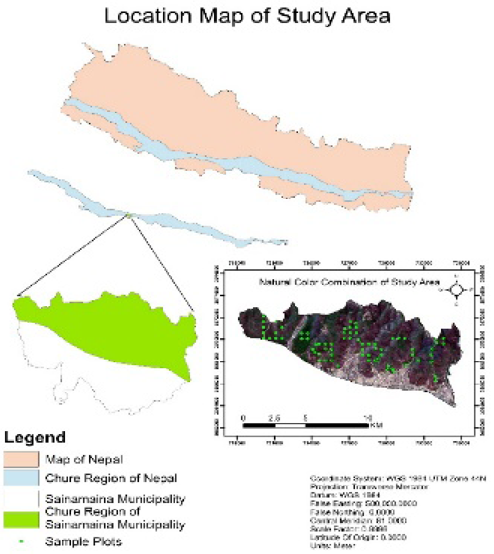

Figure 1: Location Map of Study Area

This study was conducted in Sainamaina Municipality (Fig.1). It is an area locatedin Chure region of Lumbini province in Rupandehi district of Nepal. The geographical location of study area is 83015’44’’ E to 83021’01’’ E longitude and 27038’48’’ N to 27046’05’’ N latitude. Area of Chure region of Sainamaina municipality is 9235.11 ha. The research area includes undulating topography and typical of tropical forests. Major species of this region are “Shorearobusta, Syzygiumcumini, Lagerstroemia parviflora, Mallotusphilippinensis, Anogeissus latifolia"(Poudel *et al., 2023*). The terrain slope of the study area ranges from flat land (00) to steep slopes (upto 65.70) with an elevation ranging from 95 meter to 980m above mean sea level. The average annual precipitation of 2600 mm of which 80% occurs duringmonsoon period). The mean maximum and minimum temperatures of the research areas has been recorded as 42.5°C and 7.5°C respectively(Thapa & Poudel, 2018).

Sampling strategy and field data collection

The total area of the study site is 9235.11 ha which was divided into parts within a 2 * 2 km grid Fig. 2 using ArcMap functionality. The grids were selected such that the selected grids (area 3622 ha) represented the overall vegetation of the study area. For the study, the area to be sampled was calculated using Equation 1, and the total number of sample plots to be surveyed was 72 plots which was calculated using Equation 2. Field information was gathered between the month of August and September of 2021. Circularr plots of 500m2 (12.62m radius) was employed to obtain the tree data from sample plots. Sample plots were laid in each selected grid and stratified random sampling was adopted to distribute the plots with each grid. Due to inaccessibility, some of the sample plots wereshifted to new coordinates. The species name, diameter and height of each tree with DBH 8 cm in each sample plot was measured using diameter tape and clinometer. The diameter was measure at 1.3 meters above the ground. (Askar *et al., 2018*; Maas *et al. 2008*).

$$\mathrm{SI} = \frac{a}{A} \times 100$$

$$\mathrm{n} = \frac{a}{500}$$

Where n = number of sample plots to be surveyed, a = Area to be surveyed, 500m2 is the area of the sample plot, S.I = Sampling Intensity (0.1%), and A = Total area of the study site

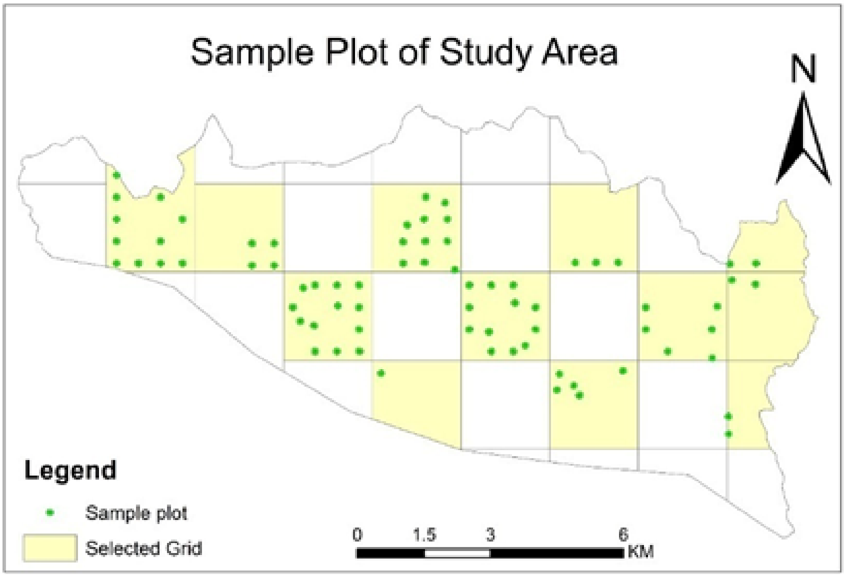

Figure 2: Grid selection and location of sample plot

Field data analysis of AGB

In this study, the aboveground biomass (AGB) was estimated using an enhanced and updated allometric equation developed by Chave et al. (2014) specifically for tropical forest trees. Chave *et al. (2014)* used an equation that incorpratеddiameter, height, and specific density of wood for biomass estimation. Height and diameter were measured on-site, whereas the specific wood density was determined through a number of literatures. Species with their default specific values (ρ) given by Khanna & Chaturvedi (1982); Thakur (2003) was used to determine tree level biomass. When specific values were unavailable, a general value (ρ= 0.674) was utilized (Pandit *et al., 2018*). The calculation of individual biomass and subsequent aggregation was done to obtain individual plot-level AGB.

$$AGB_{est} = 0.0673 * (\rho * D^2 * H)^{0.976} \qquad (3$$

Where AGBestis AGB estimated in kilogram, D is DBH in cm, H, is height in meter, ρ is wood density in g/cm3, 0.0673 and 0.976 are constants

Sentinel-2 image acquisition and processing

Sentinel-2 level 1C satellite photos (Ortho-images with UTM/WGS84, 44N projection) were downloaded from the Copernicus Scientific Hub website. The image was taken on April 20, 2021. This image was particularly chosen becauseof its low or negligible cloud cover for the period of study. The image had previously been pre-processed to the Top of the Atmosphere (TOA). Sentinel-2 level 1C was processed to level 2A using the ATCOR algorithm through the Sen2Cor plugin in Sentinels (Poudel *et al., 2023*). Application Platform (SNAP) software to produce a bottom of atmosphere (BOA) corrected reflectance image.The image other than 10 m resolution were resampled in SNAP to 10 m resolution using reference band source product “Band 2” tile with resample tool. Finally, the image was clipped for the research area in ArcMap.

Vegetation indices and extraction of pixel values

Vegetation indices (VIs) are mathematical formulas that utilize specific spectral bands to emphasize the spectral characteristics of green plants, enabling their differentiation from other features or characteristics. (Adan, 2017). It is is calculated by adding up the red spectral band (Chlorophyll absorbent) with the near-infrared band (non-absorbent). Some indices include the Short Wave Infra-Red (SWIR) band as well (Njoku, 2014). The computation is achieved by creating a linear combination of the band through the process of ratioing, differencing, and summing while also considering the ratio of differences(Hanes, 2013). A spectral transformation comprising at least two bands is used to boost the contribution of an image's vegetation features. Seven different vegetation indices were used in this study. They are Normalized Difference Vegetation Index (NDVI), Simple Ratio (SR), Soil-Adjusted Vegetation Index (SAVI), Enhanced Vegetation Index-2 (EVI2), Atmospherically Resistant Vegetation Index (ARVI), Normalized Difference Water Index (NDWI), and Normalized Difference Index 45 (NDI45) as presented in Table 5. Using the raster calculator tool in ArcGIS 10.5 software, indices were calculated incorporating image spectral bands. Using the buffer tool, a sample plot position (latitude, longitude) was exported as a 12.62 m circular plot.

Using zonal statistics and a buffered circular plot position, the pixel values for all VIs were retrieved, and the data was exported in CSV format for additional analysis.

Table 1: VIs with their formula and authors

S.No.	VIs	Authors
1.	$NDVI = \frac{\rho NIR - \rho RED}{\rho NIR + \rho RED}$	(Gitelson & Merzlyak, 1997)
2.	$SR = \frac{\rho NIR}{\rho RED}$	(Jordan 1969)
3.	$NDI45 = \frac{\rho RED\, 1 - \rho RED}{\rho RED\, 1 - \rho RED}$	(Delegido et al. 2011)
4.	$SAVI = 1.5 \times \frac{\rho NIR - \rho RED}{\rho NIR + \rho RED + 0.5}$	(Huete, 1988)
5.	$NDWI = \frac{\rho G - \rho NIR}{\rho G + \rho NIR}$	(McFeeters 1996)
6.	$ARVI = \frac{\rho NIR - \rho RED - (\rho RED - \rho BLUE)}{\rho NIR + \rho RED + (\rho RED - \rho BLUE)}$	(Kaufman and Tanre 1992)
7.	$EVI2 = 2.5 \times \frac{\rho NIR - \rho RED}{\rho NIR + 2.4 \times \rho RED + 1}$	(Jiang et al. 2008)

NIR (Near Infrared), G (Green)

Statistical analysis

SPSS and Microsoft Excel were used for statistical analysis. The relationship between each VI and AGB was calculated using linear regression models. AGB was used as the dependent variable (y) and VI was used as the independent variable (x) to determine the change in AGB as a change in VI and the value of r (correlation coefficient) and R2 (coefficient of determination) was obtained. The indices with a high value of r and R2 indicate high relation between AGB and VIs.

$Y = a + bX$,

Where, Y is AGB in t h-1, X is VIs and, a and bare parameters.

RESULTS

Descriptive statistics of field data

In the field, species enumeration and identification were also done. The results of 72 sample plots revealed a total of 929 trees. The most frequent tree species included Shorearobusta (34.33%), Bauchanania latifolia (12.80%), Anogeissus latifolia (10.22%), Terminalia alata (10.87%), Lagerstroemia parviflora (4.41%), Semecarpus anacardium (3.87%), Acacia catechu (2.47%), Mallotusphilippinensis (2.36%), and Syzygiumcumini (2.26%). The average height, DBH and AGB and CS of 929 trees was found to be 11.40 ± 0.15 meter, average = 24.20 ± 0.49

cm, 11.08 ± 0.68 t h-1 , 81.26, average = 5.17 ± 0.32 t h-1respectively. Table 2 presents species with lowest and highest AGB t h-1. Total AGB from all 72 different sample plots was found 10226.410 t h-1.

Table 2: Five species with lowest and highest AGB t/h

Five species with lowest AGB t h^{-1}		Five species with highest AGB t h^{-1}	
Species	AGB t h^{-1}	Species	AGB t h^{-1}
Diospyros malabarica	1.066	*Shorearobusta*	5903.830
Bridelia retusa	1.123	*Terminalia alata*	1890.237
Bombax cebia	1.755	*Anogeissus latifolia*	771.249
Woodfordiafruticosa	1.838	*Buchanania latifolia*	337.081
Azadirachta indica	1.915	*Lagerstroemia parviflora*	267.301

Comparative r and R^2 analysis between AGB and VIs

Comparative analysis between AGB and 7 different VIs revealed the following result as shown in Table 3. The table reveals that all Vis show positive and significant correlation between spectral indices and observed biomass($p = 0 < 0.05$). Linear model with high significant was ARVI and EVI2 model with the R^2 value of 0.7414 and 0.7415 respectively. The R^2 value indicates that about 74.14% and 74.15% of AGB per hectare was explained by linear model of model ARVI and EVI2 and that remaining about 26% was explained by other variables not introduced in the model. NDWI shows the low correlation coefficient with R^2 of 0.5539. Similarly, NDVI, SR, NDI45 and SAVI shows R^2 of 0.7122, 0.7361, 0.699 and 0.7122 respectively.

Table 3: VIs with their value of r and R^2

		NDVI	SR	NDI45	SAVI	NDWI	ARVI	EVI2
AGB	Pearson Correlation	.844**	.858**	.836**	.844**	.744**	.861**	.861**
	Sig. (2-tailezd)	0.00	0.00	0.00	0.00	0.00	0.00	0.00
	R^2	0.7122	0.7361	0.699	0.7122	0.5539	0.7414	0.7415

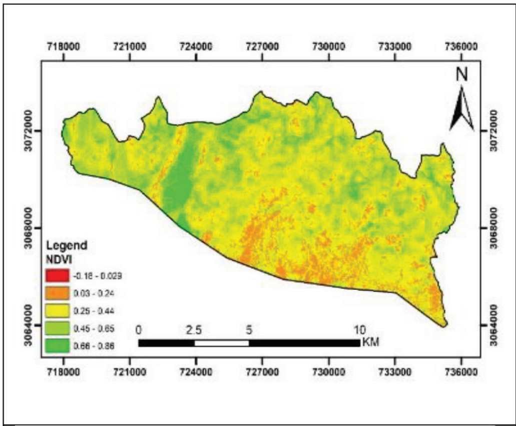

Legend
NDVI
-0.18 - 0.029
0.03 - 0.24
0.25 - 0.44
0.45 - 0.65
0.66 - 0.86
0 2.5 5 10 KM
N

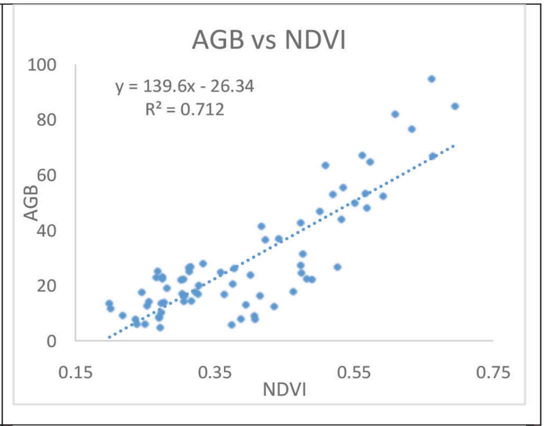

AGB vs NDVI
y = 139.6x - 26.34
R² = 0.712
AGB
NDVI

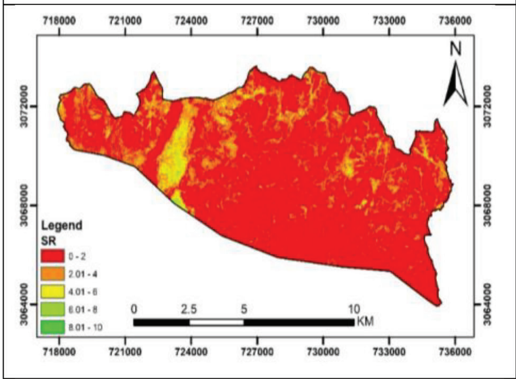

Legend
SR
0 - 2
2.01 - 4
4.01 - 6
6.01 - 8
8.01 - 10
0 2.5 5 10 KM
N

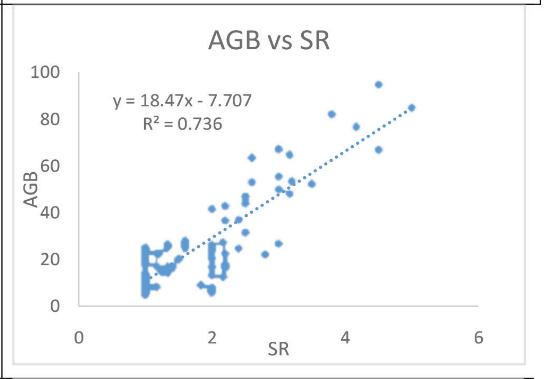

AGB vs SR
y = 18.47x - 7.707
R² = 0.736
AGB
SR

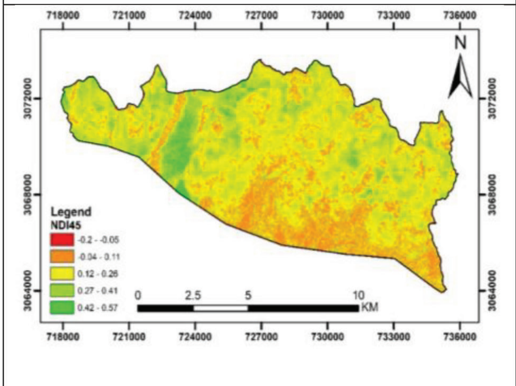

Legend
NDI45
0 2.5 5 10 KM
N

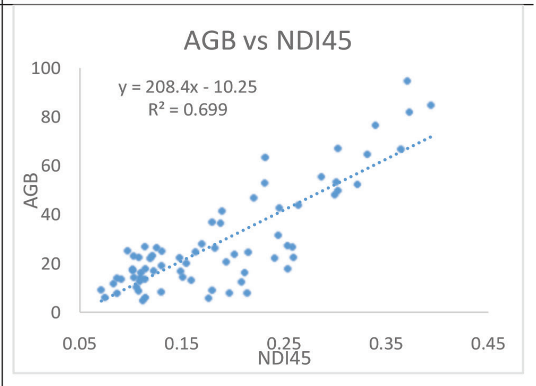

AGB vs NDI45
y = 208.4x - 10.25
R² = 0.699
AGB
NDI45

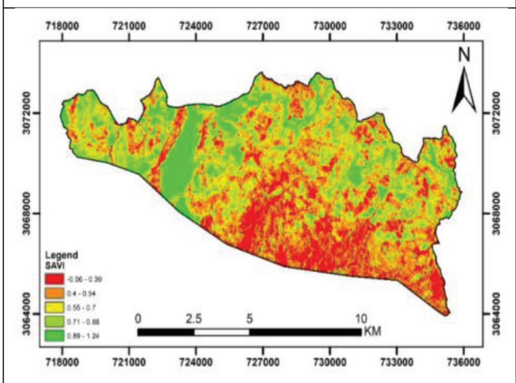

Legend
SAVI
0 2.5 5 10 KM
N

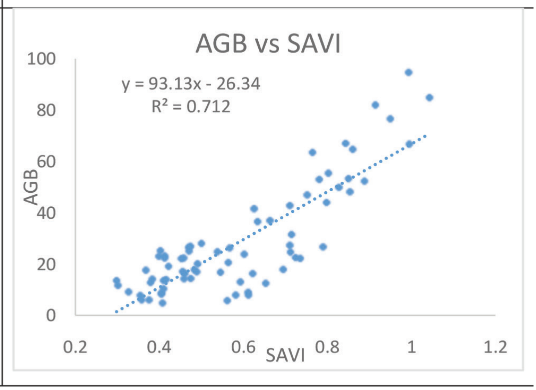

AGB vs SAVI
y = 93.13x - 26.34
R² = 0.712
AGB
SAVI

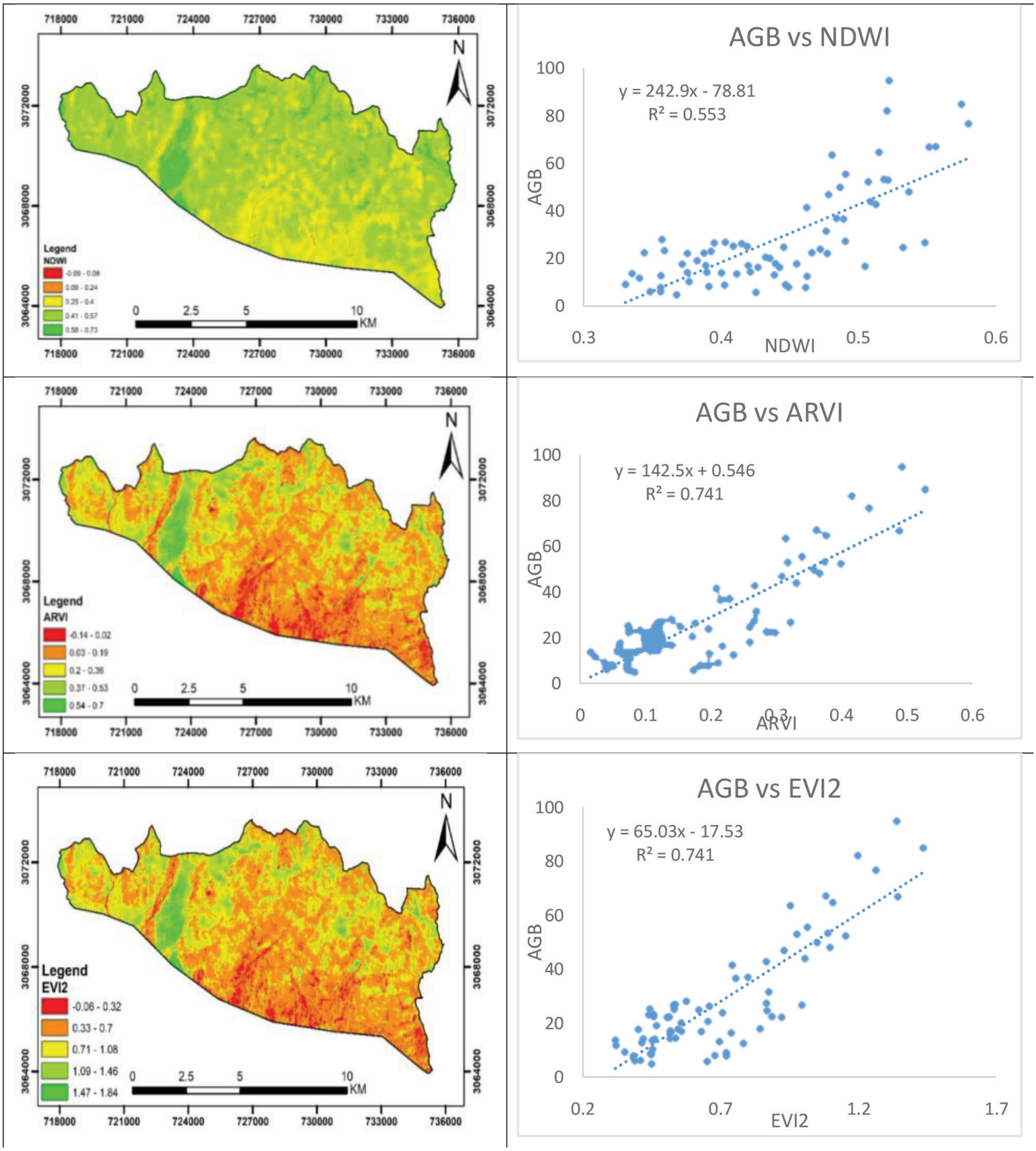

Figure 3: Computed NDVI, SR, NDI45, SAVI, NDWI, ARVI and EVI2 and relation between these VIs and AGB

Discussion

From this study, comparative analysis between the AGB and different VIs revealed that ARVI and EVI2 has strong correlation and coefficient of determination. Values of r and R^2 are 0.861 and 0.7414 respectively for ARVI while the respective value for EVI2 was 0.861 and 0.7415 atthe 5% level of significance for linear regression model. The result shows that AGB and all the VIshave strong correlation which is highly significant.

So, AGB predictive model on linear regression equation Y = 142.55x + 0.5469 for ARVI and Y = 65.03x - 17.537 for EVI2 can be suggested for predicting of AGB in Chure region.

Nakano *et al. (2013)* in their study computed 7 VIswhich are SR, NDVI, EVI, SAVI, OSAVI, LSWI and GR from reflectance data of MODIS and the result reveals that all of the vegetation indices showed significant positive correlation with measured data of AGB. Linear regression analysis indicated that SR, NDVI and OSAVI showed high correlation with AGB with R^2 = 0.777, R^2 = 0.861 and R^2 = 0.845 respectively. Joshi *et al. (2019)* in their study used slope-based vegetation indices like NDVI, Ratio, TVI and CTVI and the result showed the correlation between the VIs and AGB with correlation coefficient more than 0.7 of which NDVI had relatively higher correlation (r=0.734). The study further revealed that NDVI was relatively more significant (r = 0.734, R^2 = 0.5388 and adjusted R_2 = 0.5248) for P. roxburghiistudies. Pandit et al. (2018)gained R^2 value for SAVI, NDVI were 0.81 and 0.70 respectively while estimating the AGB in sub-tropical buffer zone community forest. Correlation value of 0.89 and 0.81 for the indices NDI45 and NDVI was obtained by (Nuthammachot *et al.* 2020) in private forest in Indonesia. Similarly, Askar *et al. (2018)* gained R^2 value of NDI45, NDVI to be 0.79 and 0.65 respectively on private forest in Indonesia using Sentinel-2. (Priatama *et al. 2022*) calculated correlation value of NDVI and SAVI to be 0.73 and 0.80 using Landsat imagery in post-mining area.

NDI45 has shown higher value of r and R2 than of NDVI which might be due to the use of red-edge region, centered at 705 (band 5), 740 (band 6), 783 (band 7), and 865 nm (band 8a). These bands have a lot of potential for monitoring various vegetation features (Shoko and Mutanga 2017). Furthermore, studies such as Askar *et al. (2018)*; Fernández-Manso *et al. (2016)*; Guo *et al. (2017)*; Nuthammachot *et al. (2020)*; Padilla *et al. (2017)* have demonstrated that red-edge VIs diminishes saturation, particularly in complex vegetation structures(Adan 2017). Saturation occurs, particularly when vegetation reaches maturity in the case of crops (Mutanga & Skidmore, 2004; Wang *et al., 2016*) while in many cases it is because of complex forest structure (Das & Singh, 2012; Lu *et al., 2016*; Sinha *et al., 2016*) causing issues in predicting forest AGB (Wernick *et al. 2021*). In such a case, the VIs is unable to detect any further increases in biomass because saturation occurs when vegetation completely covers the land, which is frequently expressed as full leaf area coverage. In this case, the biomass continues to grow while the indices remain unchanged (Adan, 2017). Steininger (2000) reported saturation at around 150 t h-1. This study concludes the average AGB from the field data to be 142.90 t h-1 which is lower than saturation amount. Thus, data saturation problem is eliminated in this study area due to lower canopy and the AGB can be predicted using the VIs consisting of the NIR, Blue and Red band i.e. ARVI and EVI2.

The degree of the relationship between VIs and AGB varies on a number of elements, including plant species and their surroundings, thus, it is possible to explain the inconsistency in the relationship between VIs and AGB to the variation in biophysical conditions of the research area (Anderson and Hanson, 1992; Mundava *et al., 2014*). As a result, depending on the local environment, one species exhibits higher connection on one VI while another on another (Joshi *et al., 2019*).

CONCLUSION

Generally, in this study Sentinel-2 VIs as ARVI and EVI2 shows potential in biomass estimation than other VIs used in this study. This study emphasizes the value of VIs in forestry-related research. Applications for this technique include management of forest resources and conservation-related projects. The use of RS techniques has made it possible to estimate biomass more quickly, more effectively, and in a timely manner for the scientific management of forest resources as opposed to the conventional methodology, which is labor-intensive, complicated, and time-consuming. Thus, freely available multispectral Sentinel-2 data with high spatial, temporal resolution are suitable for calculating AGB at a small scale over wide areas.

ACKNOWLEDGEMENTS:

The authors would like to express sincere thanks to the independent reviewers for providing useful comments and suggestions to improve the quality of the manuscript. Our gratitude goes to Krishi Ban Prabardhan for providing the fund to conduct this study. Mr. Megh Bahadur Saru, local resource person whodeserves a particular mention for teaming with us while we were gathering field level data.

REFERENCES

Alkama, R., &Cescatti, A. (2016). *Biophysical climate impacts of recent changes in global forest cover.* Science, 351(6273), 600–604. https://doi.org/10.1126/science.aac8083.

Adan, M. S.(2016) *Master of science* University of Twente Forestry, Pokhara, Nepal. M.Sc. Thesis.

Anderson, G. L., & Hanson, J. D. (1992). *Evaluating hand-held radiometer derived vegetation indices for estimating above ground biomass.* Geocarto International, 7(1), 71–78. https://doi.org/10.1080/10106049209354354.

Askar, Nuthammachot, N., Phairuang, W., Wicaksono, P., & Sayektiningsih, T. (2018). *Estimating Aboveground Biomass on Private Forest Using Sentinel-2 Imagery.* Journal of Sensors, 2018, 1–11. https://doi.org/10.1155/2018/6745629.

Astola, H., Häme, T., Sirro, L., Molinier, M., & Kilpi, J. (2019). *Comparison of Sentinel-2 and Landsat 8 imagery for forest variable prediction in boreal region.* Remote Sensing of Environment, 223, 257–273. https://doi.org/10.1016/j.rse.2019.01.019.

Attarchi, S., & Gloaguen, R. (2014). *Improving the Estimation of Above Ground Biomass Using Dual Polarimetric PALSAR and ETM+ Data in the Hyrcanian Mountain Forest (Iran).* Remote Sensing, 6(5), 3693–3715. https://doi.org/10.3390/rs6053693.

Basuki, T. M., Van Laake, P., Skidmore, A. K., & Hussin, Y. A. (2009). *Allometric equations for estimating the above-ground biomass in tropical lowland Dipterocarp forests.* Forest Ecology and Management, 257(8), 1684–1694. https://doi.org/10.1016/j.foreco.2009.01.027.

Biswas, S., Huang, Q., Anand, A., Mon, M. S., Arnold, F., & Leimgruber, P. (2020). *A Multi Sensor Approach to Forest Type Mapping for Advancing Monitoring of Sustainable Development Goals (SDG) in Myanmar.* Remote Sensing, 12(19), 3220. https://doi.org/10.3390/rs12193220

Boyd, D. S. (1999). *The relationship between the biomass of Cameroonian tropical forests and radiation reflected in middle infrared wavelengths (3.0-5.0 mu m).* International Journal of Remote Sensing, 20(5), 1017–1023. https://doi.org/10.1080/014311699213055

Chave, J., Réjou-Méchain, M., Búrquez, A., Chidumayo, E. N., Colgan, M. S., Delitti, W. B. C., . . . Vieilledent, G. (2014). *Improved allometric models to estimate the aboveground biomass of tropical trees. Global Change Biology,* 20(10), 3177–3190. https://doi.org/10.1111/gcb.12629.

Das, S., & Singh, T. P. (2012). *Correlation analysis between biomass and spectral vegetation indices of forest ecosystem.* Int. J. Eng. Res. Technol, 1(5), 1-13. doi: 10.17577/IJERTV1IS5369.

Delegido, J., Verrelst, J., Alonso, L., & Moreno, J. (2011). *Evaluation of Sentinel-2 Red-Edge Bands for Empirical Estimation of Green LAI and Chlorophyll Content. Sensors*, 11(7), 7063–7081. https://doi.org/10.3390/s110707063.

Fernández-Manso, A., Fernández-Manso, O., & Quintano, C. (2016). *SENTINEL-2A red-edge spectral indices suitability for discriminating burn severity.* International Journal of Applied Earth Observation and Geoinformation, 50, 170–175. https://doi.org/10.1016/j.jag.2016.03.005.

Foody, G. M., Boyd, D. S., & Cutler, M. E. J. (2003). *Predictive relations of tropical forest biomass from Landsat TM data and their transferability between regions.* Remote Sensing of Environment, 85(4), 463–474. https://doi.org/10.1016/s0034-4257(03)00039-7.

Forkuor, G., Dimobe, K., Serme, I., & Tondoh, J. E. (2017). *Landsat-8 vs. Sentinel-2: examining the added value of sentinel-2's red-edge bands to land-use and land-cover mapping in Burkina Faso.* Giscience & Remote Sensing, 55(3), 331–354. https://doi.org/10.1080/15481603.2017.1370169.

Gitelson, A. A., & Merzlyak, M. N. (1997). *Remote estimation of chlorophyll content in higher plant leaves.* International Journal of Remote Sensing, 18(12), 2691–2697. https://doi.org/10.1080/014311697217558.

Guo, B., Qi, S., Heng, Y., Duan, J., Zhang, H., Wu, Y., . . . Zhu, Y. (2017). *Remotely assessing leaf N uptake in winter wheat based on canopy hyperspectral red-edge absorption.* European Journal of Agronomy, 82, 113–124. https://doi.org/10.1016/j.eja.2016.10.009.

Hanes, J. (2013). *Biophysical Applications of Satellite Remote Sensing.* Springer Science & Business Media.

He, C., Zhang, Q., Li, Y., Li, X., & Shi, P. (2005). *Zoning grassland protection area using remote sensing and cellular automata modeling—A case study in Xilingol steppe grassland in northern China.* Journal of Arid Environments, 63(4), 814–826. https://doi.org/10.1016/j.jaridenv.2005.03.028

Heiskanen, J. (2006). *Estimating aboveground tree biomass and leaf area index in a mountain birch forest using ASTER satellite data.* International Journal of Remote Sensing, 27(6), 1135–1158. https://doi.org/10.1080/01431160500353858.

Huete, A. (1988). *A soil-adjusted vegetation index (SAVI).* Remote Sensing of Environment, 25(3), 295–309. https://doi.org/10.1016/0034-4257(88)90106-x. THIS REFERENCE APPEARS in TABLE 1

Hurcom, S., & Harrison, A. (1998). *The NDVI and spectral decomposition for semi-arid vegetation abundance* *estimation.* International Journal of Remote Sensing, 19(16), 3109–3125. https://doi.org/10.1080/014311698214217.

Jiang, Z., Huete, A., Didan, K., & Miura, T. (2008). *Development of a two-band enhanced vegetation index without a blue band.* Remote Sensing of Environment, 112(10), 3833–3845. https://doi.org/10.1016/j.rse.2008.06.006.

Jordan, C. F. (1969). *Derivation of Leaf-Area Index from Quality of Light on the Forest Floor.* Ecology, 50(4), 663–666. https://doi.org/10.2307/1936256.

Joshi, A., Shahnawaz, S., & Ranjit, B. (2019). *ESTIMATING ABOVE GROUND BIOMASS OF <i>PINUS ROXBHURGHII</i> USING SLOPE BASED VEGETATION INDEX MODEL.* ISPRS Annals of the Photogrammetry, Remote Sensing and Spatial Information Sciences, IV-5/W2, 35–42. https://doi.org/10.5194/isprs-annals-iv-5-w2-35-2019.

Kankare, V., Vastaranta, M., Holopainen, M., Räty, M., Yu, X., Hyyppä, J., . . . Viitala, R. (2013). *Retrieval of Forest Aboveground Biomass and Stem Volume with Airborne Scanning LiDAR.* Remote Sensing, 5(5), 2257–2274. https://doi.org/10.3390/rs5052257.

Kaufman, Y. J., & Tanré, D. (1992). *Atmospherically resistant vegetation index (ARVI) for EOS-MODIS.* IEEE Transactions on Geoscience and Remote Sensing, 30(2), 261–270. https://doi.org/10.1109/36.134076.

Khanna, L. S., &Chaturvedi, A.N.(1982). *Forest Mensuration.* International Book Distributors.

Kumar, L., Sinha, P., Taylor, S., & Alqurashi, A. F. (2015). *Review of the use of remote sensing for biomass estimation to support renewable energy generation.* Journal of Applied Remote Sensing, 9(1), 097696. https://doi.org/10.1117/1.jrs.9.097696.

Li, C., Zhou, L., & Xu, W. (2021). *Estimating Aboveground Biomass Using Sentinel-2 MSI Data and Ensemble Algorithms for Grassland in the Shengjin Lake Wetland, China.* Remote Sensing, 13(8), 1595. https://doi.org/10.3390/rs13081595.

Lourenço, P. (2021). *Biomass estimation using satellite-based data.* In Forest Biomass-From Trees to Energy. IntechOpen. doi: 10.3390/s110707063.

Lu, D. (2006). *The potential and challenge of remote sensing-based biomass estimation.* International Journal of Remote Sensing, 27(7), 1297–1328. https://doi.org/10.1080/01431160500486732.

Lu, D., Chen, Q., Wang, G., Liu, L., Li, G., & Moran, E. F. (2014). *A survey of remote sensing-based aboveground biomass estimation methods in forest ecosystems.* International Journal of Digital Earth, 9(1), 63–105. https://doi.org/10.1080/17538947.2014.990526.

Maas, H., Bienert, A., Scheller, S., & Keane, E. (2008). *Automatic forest inventory parameter determination from terrestrial laser scanner data.* International Journal of Remote Sensing, 29(5), 1579–1593. https://doi.org/10.1080/01431160701736406.

Mauya, E. W., Ene, L. T., Gobakken, T., Næsset, E., Malimbwi, R. E., & Zahabu, E. (2015). *Modelling aboveground forest biomass using airborne laser scanner data in the miombo woodlands of Tanzania.* Carbon Balance and Management. https://doi.org/10.1186/s13021-015-0037-2.

Maynard, C., Lawrence, R. L., Nielsen, G. A., & Decker, G. (2007). *Modeling Vegetation Amount Using Bandwise Regression and Ecological Site Descriptions as an Alternative to Vegetation Indices.* Giscience & Remote Sensing, 44(1), 68–81. https://doi.org/10.2747/1548-1603.44.1.68.

McFeeters, S. K. (1996). *The use of the Normalized Difference Water Index (NDWI) in the delineation of open water features.* International Journal of Remote Sensing, 17(7), 1425–1432. https://doi.org/10.1080/01431169608948714.

Mundava, C., Helmholz, P., Schut, A. G. T., Corner, R. J., McAtee, B., & Lamb, D. (2014). *Evaluation of vegetation indices for rangeland biomass estimation in the Kimberley area of Western Australia.* ISPRS Annals of the Photogrammetry, Remote Sensing and Spatial Information Sciences, II–7, 47–53. https://doi.org/10.5194/isprsannals-ii-7-47-2014

Mutanga, O., & Skidmore, A. K. (2004). *Hyperspectral band depth analysis for a better estimation of grass biomass (Cenchrus ciliaris) measured under controlled laboratory* *conditions.* International Journal of Applied Earth Observation and Geoinformation, 5(2), 87–96. https://doi.org/10.1016/j.jag.2004.01.001.

Nakano, T., Bavuudorj, G., Urianhai, N. G., & Shinoda, M. (2013). *Monitoring aboveground biomass in semiarid grasslands using MODIS images.* Journal of Agricultural Meteorology, 69(1), 33–39. https://doi.org/10.2480/agrmet.69.1.1.

Njoku, E. G. (Ed.). (2014). *Encyclopedia of remote sensing (pp. 344-348)*. Springer New York.

Nunes LJR, Meireles CIR, Pinto Gomes CJ, Almeida Ribeiro NMC (2020). *Forest Contribution to Climate Change Mitigation: Management Oriented to Carbon Capture and Storage.* Climate, 8(2):21. https://doi.org/10.3390/cli8020021

Nuthammachot, N., Askar, A., Stratoulias, D., & Wicaksono, P. (2020). *Combined use of Sentinel-1 and Sentinel-2 data for improving above-ground biomass estimation.* Geocarto International, 37(2), 366–376. https://doi.org/10.1080/10106049.2020.1726507.

Padilla, F. M., Peña-Fleitas, M. T., Gallardo, M., & Thompson, R. L. (2017). *Determination of sufficiency values of canopy reflectance vegetation indices for maximum growth and yield of cucumber.* European Journal of Agronomy, 84, 1–15. https://doi.org/10.1016/j.eja.2016.12.007.

Pan, Y., Birdsey, R. A., Phillips, O. L., & Jackson, R. B. (2013). *The Structure, Distribution, and Biomass of the World's Forests.* Annual Review of Ecology, Evolution, and Systematics, 44(1), 593–622. https://doi.org/10.1146/annurev-ecolsys-110512-135914.

Pandit, S., Tsuyuki, S., & Dube, T. (2018). *Estimating Above-Ground Biomass in Sub-Tropical Buffer Zone Community Forests, Nepal, Using Sentinel 2 Data.* Remote Sensing, 10(4), 601. https://doi.org/10.3390/rs10040601.

Poudel, A., Shrestha, H. L., Mahat, N., Sharma, G., Aryal, S., Kalakheti, R., & Lamsal, B. (2023). *Modeling and Mapping of Aboveground Biomass and Carbon Stock Using Sentinel-2 Imagery in Chure Region, Nepal.* International Journal of Forestry Research, 2023, 1–12. https://doi.org/10.1155/2023/5553957.

Priatama, A. R., Setiawan, Y., Mansur, I., & Masyhuri, M. (2022). *Regression Models for Estimating Aboveground Biomass and Stand Volume Using Landsat-Based Indices in Post-Mining Area.* Journal of Tropical Forest Management/ Jurnal Manajemen Hutan Tropika, 28(1). 1–14. https://doi.org/10.7226/jtfm.28.1.1.

Qiu, S., He, B., Yin, C. C., & Liao, Z. (2017). *Assessments of sentinel-2 vegetation red-edge spectral bands for improving land cover classification.* The International Archives of the Photogrammetry, Remote Sensing and Spatial Information Sciences, XLII-2/W7, 871–874. https://doi.org/10.5194/isprs-archives-xlii-2-w7-871-2017

Rahman, A. F., Gamon, J. A., Sims, D. B., & Schmidts, M. (2003). *Optimum pixel size for hyperspectral studies of ecosystem function in southern California chaparral and grassland.* Remote Sensing of Environment, 84(2), 192–207. https://doi.org/10.1016/s0034-4257(02)00107-4.

Schlerf, M., Atzberger, C., & Hill, J. (2005). *Remote sensing of forest biophysical variables using HyMap imaging spectrometer data.* Remote Sensing of Environment, 95(2), 177–194. https://doi.org/10.1016/j.rse.2004.12.016.

Shoko, C., & Mutanga, O. (2017). *Examining the strength of the newly-launched Sentinel 2 MSI sensor in detecting and discriminating subtle differences between C3 and C4 grass species.* Isprs Journal of Photogrammetry and Remote Sensing, 129, 32–40. https://doi.org/10.1016/j.isprsjprs.2017.04.016.

Sinha, S., Jeganathan, C., Sharma, L., Nathawat, M. S., Das, A., & Mohan, S. (2016). *Developing synergy regression models with space-borne ALOS PALSAR and Landsat TM sensors for retrieving tropical forest biomass.* Journal of Earth System Science, 125(4), 725–735. https://doi.org/10.1007/s12040-016-0692-z.

Steininger, M. K. (2000). *Satellite estimation of tropical secondary forest above-ground biomass: Data from Brazil and Bolivia.* International Journal of Remote Sensing, 21(6–7), 1139–1157. https://doi.org/10.1080/014311600210119.

Temesgen, H., Affleck, D. L. R., Poudel, K. C., Gray,

A. R., & Sessions, J. (2015). *A review of the challenges and opportunities in estimating above ground forest biomass using tree-level models.* Scandinavian Journal of Forest Research, 1–10. https://doi.org/10.1080/02827581.2015.1012114

Thakur, R. B. (2003). *A Compendium of Tree Species of Nepal.* Mr. & Mrs. RB Thakur.

Thapa, M., & Poudel, G. (2018). *Assessing the Coverage of Urban Green Space in Butwal Sub-Metropolitan City, Nepal: A GIS based Approach.* Forestry, 15, 77–86. https://doi.org/10.3126/forestry.v15i0.24923

Utari, D., Kamal, M., & Sidik, F. (2020). *Above-ground biomass estimation of mangrove forest using WorldView-2 imagery in Perancak Estuary, Bali.* In IOP Conference Series: Earth and Environmental Science (Vol. 500, No. 1, p. 012011). IOP Publishing.

Wahlang, R., & Chaturvedi, S. (2020). *Relationship Between Above-Ground Biomass and Different Vegetation Indices of Forests of Ri-Bhoi District, Meghalaya, India.* International Journal of Engineering Research And, V9(05). https://doi.org/10.17577/ijertv9is050128.

Wang, C., Feng, M., Yang, W., Ding, G., Sun, H., Liang, Z., . . . Qiao, X. (2016). *Impact of spectral saturation on leaf area index and aboveground biomass estimation of winter wheat.* Spectroscopy Letters, 49(4), 241–248. https://doi.org/10.1080/00387010.2015.1133652.

Wannasiri, W., Nagai, M., Honda, K., Santitamnont, P., & Miphokasap, P. (2013). *Extraction of Mangrove Biophysical Parameters Using Airborne LiDAR.* Remote Sensing, 5(4), 1787–1808. https://doi.org/10.3390/rs5041787.

Wernick, I. K., Ciais, P., Fridman, J., Högberg, P., Korhonen, K. T., Nordin, A., & Kauppi, P. E. (2021). *Quantifying forest change in the European Union.* Nature, 592(7856), E13–E14. https://doi.org/10.1038/s41586-021-03293-w